JETIR.ORG ISSN: 2349-5162 | ESTD Year : 2014 | Monthly Issue
JOURNAL OF EMERGING TECHNOLOGIES AND INNOVATIVE RESEARCH (JETIR)
An International Scholarly Open Access, Peer-reviewed, Refereed Journal

Vortex pinning and Effective pinning energy inside the crust of Neutron Star

M. K. Maurya[1], Harleen Babara[2], Sunil Kumar Gupta[3], , Shailesh Kumar Dewangan[4]
[1, 2]Department of Physics, Rajeev Gandhi Government P.G. College, Ambikapur-497001, Chhattisgarh, India
[2]Student Department of Physics, Rajeev Gandhi Government P.G. College, Ambikapur-497001, Chhattisgarh, India
[3]Department of Mathematics, Govt. Rajmohinidevi Girls P.G. College, Ambikapur-497001, Chhattisgarh, India
[4]Department of Physics, Shri, Sai Baba Aadarsh Mahavidyalay , Ambikapur-497001, Chhattisgarh, India

Abstract

We study the motion of pinning of superfluid vortices inside the inner crust of neutron star. The pinning occurring in NS crust is assumed to be of certain lattice orientation of an ideal body centered cubic lattice. Here, we tend to solely examine the interaction between nuclei within the vortex line for Nuclear and Interspatial pinning withinfive different regions of superfluid crust. The angular momentum for the superfluid neutronsis in the form of array of quantized vortices. Furthermore, when these vortices are pinned to the nuclear lattice, it restricts the superfluid from spinning down along with storing the angular momentum which when released causes pulsar glitches. During this paper, we tend to investigate the role of drag parameter, capture radius and coherence length for vortex-nucleus interaction throughout the two pinning actions and study the variation in effective pinning energy for the five different regions within superfluid crustwith respect to pinning energy per pinning site.

Keywords: Dense matter – stars: neutron – pulsars: general- star: rotation-superfluidity vortex.

1. Introduction:

The mechanism for superconductivity in terrestrial materials as a result of the BSC theory and the observation of the glitches in the timing data of Vela pulsar [1] motivates the concept that the neutron stars contain a liquid interior of superfluid neutrons and superconducting protons [2]. Possibly, in neutron stars vortex pinning interaction plays an important role since the dynamics of various condensed superfluid systems [3], vortices quantization can have an observable impact. For example, a suddenunpinningof vortices increases the rotation frequencies of neutron stars in pulsar glitches [4-6]. When superfluid and normal components of a pulsar rotate at the same angular frequency, it is said to be in equilibrium. Due to magnetic radiation, the pulsar losses its angular momentum by reducing the pulsation rate and this gradually slows down the crust of nuclear star. The superfluid must also release the angular momentum by weakening the vortex concentration to maintain the equilibrium. There will be a rapid increase in pulsation rate inside the glitches due to the presence of pinning sites (nuclei, lattices sites, defects, etc.,) that may restrict the vortex motion by building up the stress until a large number of vortices rapidly unpin and is weakened by transferring their angular momentum to the crust. Even after 40 years of this mechanism, it is still obscure to us.The basic image has the angular momentum held on by the neutron superfluid in the crust, with pinning provided by nuclei command in an exceeding lattice by the electrostatic (Coulombic) interaction.Recent results recommend that the crystal neutrons might not support enough angular

momentum to clarify discovered neutron star glitches [7], during which case the interaction between neutron superfluid vortices and proton flux tubes within the outer core [8] or quark matter phases in the core might play a role [9]. In either case, vortex pinning interactions can be a reliable technique key [10]. During this paper, we tend to specialize in the relation between effective interaction energy and pinning energy per pinning site within pulsar glitches.Glitches are the unexpected increase in frequency (instantaneous to the accuracy of the data) of an otherwise swiftly spinning down radio pulsar.After the event, in several cases, there is a rise within the spin-down rate that relaxes exponentially back to the pre-glitch spin-down [11].Soon after the first observations, the terribly long-time scales regarding this relaxation (up to months) were related to the re-coupling of a loosely coupled superfluid component inside the nuclear star crust [12].A vital side of superfluid dynamics is that the nucleon condensation will solely rotate by forming an array of quantized vortices, that describes a mean rotation rate for the fluid. Vorticity must be restricted for the superfluid to spin down. If the vortices are pinned or strongly attached to the ions inside the crust, their motion is prevented and superfluid cannot follow the spin-down of the crust and this causes angular momentum to be stored and laterreleased or unpinning it catastrophically during a glitch[13].The effective pinning interaction energy of a vortex depends, however, on the mesoscopic interaction between the vortex and lots of pinning sites, and so on the rigidity of the vortex, on its radius (represented by the superfluid coherence length ζ) and on the lattice spacing.This naturally ends up in the likelihood of various pinning regimes in several regions of the crust.Alpar et al. [14-19] understood the slow post-glitch recovery of the Vela neutron star in terms of vortex 'creep', i.e., the thermally activated movement of pinned vortices, and distinguished it between three regimes: strong, weak, and super weak pinning.

The various regimes rely upon the interaction between the quantities mentioned earlier: in strong pinning, the coherence length ζ of a vortex is smaller than the lattice spacing, and therefore the interaction is robust enough to displace nuclei, whereas within the weak pinning regimethis will benot the case. On the other hand, super weak pinning is experienced when the coherence length ζis larger than the lattice spacing and a vortex can enclose many nuclei. Thus, there is no preferred configuration for pinning during this case, because as the vortex moves there will be very little change in the energy. When pinning force is said to be weak and within the limit of infinitely long vortices, then all the configurations are equal and there would be no pinning [20-21].The theoretical calculations of the mesoscopic pinning force relied, however, on estimates in the weak pinning case for the particular configuration of vortices aligned with the crystal axis. Though little is thought regarding the defect structure of the crust, one will not, in general, expect the space lattice to be directed within the same direction over the full length of a vortex. Recently, Link [22] have performed simulations of the motion of a vortex during a three-dimensional random potential, and located that the rigidity of the vortex does, indeed, play an essential role in settingthe limit of superfluid flow after which the vortices are unpinned [23].

2.Theoretical Description:

Theconcept of a neutron star crust is to shape a crystal where absolutely ionized neutron-rich nuclei shape a body-centered cubic (BCC) lattice. In this configuration, every nucleus is on the center of a cubic cell of aspect s = 2 R_{ws} with nuclei at every vortex. The separation among the ions (i.e., the potential pinning sites) consequently relies upon R_{ws}, the radius of the Wigner–Seitz cell, that is a function of the density ρ_{ws}. In our calculation, we use the classic effects from Negele &Vautherin [5] where the crust is split into five zones, individual zone characterised through a particular value of R_{ws} and R_N, that is the radius of the nucleus that occupies a single site of the lattice [23]. To calculate the effective pinning pressure, we must discover the configurations where the vortex is maximum strongly pinned to the lattice and the configurations where it is 'unfastened' (be aware that a vortex is by no means genuinely unfastenedbecause it will continually intersect pinning centers). The 'unfastened' or free configuration represents the average energy configuration among places of maximum pinning. Once this has been done, the maximum pinning pressureF_P follows from

$$F_P = \frac{E_{free} - E_p}{\Delta r} \qquad (1)$$

WhereE_p is that the energy of the foremost powerfully pinned configuration and $E_{free}$is the energy of the free configuration. The average distance the vortex needs to move between the configuration energy of a specific number configuration can depend upon the quantity of ions that it is able to pin to. Intuitively, the additional sites it will pin to, the bigger the energy gain, the stronger the pinning. So as to perform the calculation, it is, therefore, necessary to contemplate the pinning energy per pinning site E_{Pin}, i.e., the amount by which the energy of the systemis modifiedonce a nucleus is within the vortex. This amount depends on the competition between the kinetic energy and also the condensation energy of the superfluid, which is powerfully density-dependent and can therefore change if a dense nucleus is introduced within the vortex. During this work, we tend to use the results of Donati& Pizzochero [30-33], who calculatedE_{Pin}systematically in the native density approximation. We can see here that in some regions E_{Pin} is positive, i.e., it tends energy to introduce a nucleus in an exceeding vortex. In these regions, the vortex–nucleus interaction is repulsive and one has 'interspatial' pinning (IP), during which the favoured vortex configurations are intermediate nuclei. We then deal with the case in which the interaction between nuclei and vortices is enticing or attractive i.e., 'nuclear' pinning (NP). The parameter β refers to the suppression value for the nuclear pairing gap applied in the calculations:$\Delta = \frac{\Delta_0}{\beta}$,where $\Delta_0$is that the pairing gap of the superfluid,obtained by using the vacant interaction. This factor is said to be the polarization effects of matter on the nuclear interaction.Here, the non-polarized interaction case is described by β =1 while the polarized interaction result is given by β =3.For β = 1, the mean pairing gap incorporates a maximum of 3 MeV, which corresponds to the strong pairing situation, whereas for β = 3 the mean pairing gap has a maximum of about 1 MeV, as sometimes assumed within the weak pairing scenario [23]. Realistic Monte Carlo simulations of nucleon matter [34] indicate a reduction of the pairing gap according to the selection of β = 3. The entire energy of the interaction between a given vortex portion and the lattice is calculated summing the contribution of every nucleus that may be captured by the pinning force. Naively, this might be done by considering the vortex as a cylinder of radius ζ and calculating what percentage of nuclei are contained inside it. This information indicates towards the attainable deformation of the nuclear lattice. The lattice has elastic properties;thus,it is possible for nuclei to be displaced from their equilibrium position below the action of the pinning pressure [23]. The resultant energy per-site in the cylinder can be expressed as

$$E(r) = E_{pin} + E_1(r) \qquad (2)$$

where r is the distance of the vortex axis from the equilibrium position of the particular nucleus. During this approach, the pinning energy per site E_{pin} is corrected by the value$E_1(r)$ that encodes the modification in electrostatic energy because of the displacement of the nucleus. We are going to then outline the capture radiusr_{cap} because this is the radius inside which it is energetically favorable for the nuclei to be displaced: this may be the radius of the vortex to be utilized in the investigating procedure. Allowing us to currently estimate$r_{cap}$for each NP and IP [23].

2.1 Nuclear pinning:

Within the NP regime (E_{pin}<0) pinning region can be defined by assuming that a nucleus contributes to the total interaction by a factor E_{pin} if it is completely inside the vortex: that is, its distance from the vortex axismust be less than α= ζ− R_N (Fig. 1),with α= 0 ifζ< R_N. If the distance of a site is r>αfrom the vortex axis, the nucleus should be dragged by a distance δ(r) = r-α.The electrostatic energy is calculated ingeneral form using Gauss theorem along with the Wigner–Seitz approximation, that divides the lattice into free space of spherical cells of radius R_{WS}, each with an ion within the centre enclosed by the electron and neutron gas:

$$E_1(r) = \frac{Z^2 e^2}{2R_{ws}^3}\delta^2(r)\,, \qquad (3)$$

where e is the elementary charge and Z is the number of protons and electrons in the cell.Since, all those nuclei whose equilibrium position is already within the pinning region does notget to be dragged,therefore there is no

electrostatic term in its energy(E(r) =E_{pin}if r <α). We can currently outline the maximum drag distancer_d because the value of δ(r) with respect to the effective pinning interaction of equation (2) becomes zero:

$$r_d = \sqrt{\frac{2E_{pin}{R_{ws}}^3}{Z^2e^2}} \quad (4)$$

According to this condition, the final capture radiusr_{cap}must be given by:

$$r_{cap} = \alpha + r_d = \zeta - R_N + r_d, \quad (5)$$

For the calculation of total interaction energy between a particular vortex segment (of length L) and lattice, the contribution of each captured nucleus is sum together. This energy is calculated by using an integral over a uniform distribution of nuclei, that is valid for the variety of nuclei that are taken into consideration turns into very large, so for L≫Rws. Given N the number of pinning sites that fall inside a cylinder of radius r_{cap} and lengthL, the superficial density will be $n_N = \frac{N}{\pi r_{cap}^2}$.

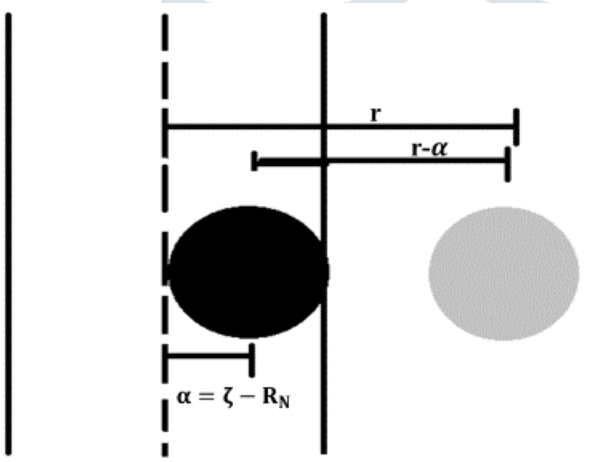

Figure (1): Diagram of a nucleus displacement (NP case). The white and black circles represent, respectively, the starting and final position of the nucleus. The dashed line represents the displacement *δ*(*r*).

Then the total energy is calculated as

$$E = \int_0^{\alpha} E_{pin}\, n_S 2\pi r dr + \int_{\alpha}^{\alpha+\alpha_0} (E_{pin} + E_1(r))\; n_S 2\pi r dr\,,$$

$$= \frac{NE_{pin}}{(\alpha+\alpha_0)^2}\left(\alpha^2 + \frac{4}{3}\alpha r_d + \frac{1}{2}{r_d}^2\right). \quad (6)$$

From this equation, we are able to directly measure the effective interaction energy per site E_{in}, outlined by $E=NE_{in}$:

$$E_{in} = \frac{E_{pin}}{(\alpha+\alpha_0)^2}\left(\alpha^2 + \frac{4}{3}\alpha r_d + \frac{1}{2}{r_d}^2\right). \quad (7)$$

2.2 Interspatial pinning:

The analysis of r_{cap} andE_{in} within the IP regime (E_{pin}> 0) follows a similar step of the previous section, however taking under considerationthat during this case the interaction is repulsive and hence a nucleus that lies in the vortex core should be expelled rather than dragged into it to lower the energy. A nucleus is said to be expelled or released if it is completely outside the vortex, which is possible when its distance from the vortex axis is larger than $\alpha = \zeta + R_N$(Fig. 2).A nucleus that is expelled will not contribute to the pinning energy.

Then the drag distance is given by δ(r) =α – r and maximum value of r_d, is given by the energy $E_{pin} = E_1(\alpha = r_d)$. This determinesthat the nuclear displacement happens onlywhen the energy of the dragged nucleus

configuration is less than the energy of the configuration wherever the nucleus continues to be in its equilibrium position within the lattice:

$$r_d = \sqrt{\frac{2E_{pin}{R_{ws}}^3}{Z^2e^2}} \tag{8}$$

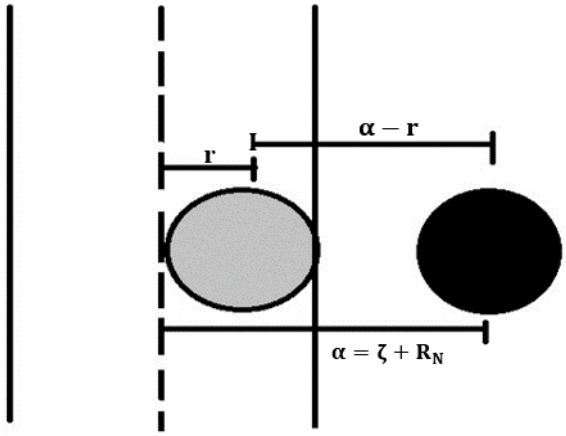

Figure (2):Diagram of a nucleus displacement (IP case). The white and black circles represent, respectively, the starting and final position of the nucleus. The dashed line represents the displacement $\delta(r)$.

In this case, the value of capture radius for the counting procedureмust be equal to α. This is because only those nuclei that lies in the pinning region can contribute to the pinning energy,

$$r_{cap} = \alpha = \zeta - R_N, \tag{9}$$

Then, if $r_d<\alpha$, the total energy is calculated as

$$E = \int_0^{\alpha-\alpha_0} E_{pin}\, n_S 2\pi r dr + \int_{\alpha-\alpha_0}^{\alpha} E_1(r)\, n_S 2\pi r dr\,, \tag{10}$$

since, thenuclei in this region have been expelled therefore second term of the integral contains only the electrostatic contribution. In case of$r_d>\alpha$, all the nuclei that contribute to the pinning energy are dragged outside the vortex: then, we can write

$$E = \int_0^{\alpha} E_1(r)\, n_S 2\pi r dr. \tag{11}$$

By evaluating these integrals and determining again$E=NE_{in}$, we get the effective pinning energy per site

$$\mathrm{E_{in}} = \begin{cases} E_{pin}\left(\alpha^2 + \frac{4}{3}\alpha r_d + \frac{1}{2}{r_d}^2\right) & r_d \le \alpha \\ E_{pin}\frac{\alpha^2}{6{r_d}^2} & r_d > \alpha \end{cases} \tag{12}$$

2.3 Vortex length:

The vortex is said to be straight for the cylinder of the length L which is determined by the counting procedure.Based oncalculated energy we can describe the range of the magnitude of L(the discussion was generated within the NP regime; however, a similar result was obtained in the IP regime). If the vortex, tension T

(self-energy per unit length), will bend under the influence of the pinning force, we can equate the energy of two limiting configurations: the straight (infinitely rigid) vortex (Fig.3.1) and also, the vortex that has bent so as to pin to an extra nucleus at a typical distance of the order of R_{ws}(Fig. 3.2):

$$T_L = E_{pin} + T(L + \Delta L) \quad (13)$$

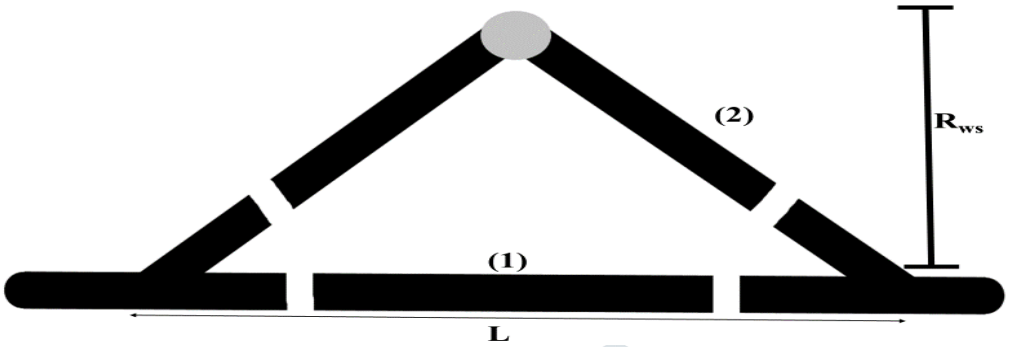

Figure (3): Diagram of the vortex deformation. We have drawn two different shapes to show vortex deformation: a rigid vortex (1) and a bent vortex (2). Lis the vortex length and $R_{ws}$is the Wigner–Seitz radius.

The difference ΔLof the vortex length in the two configurations is obviously

$$\Delta L = 2\sqrt{\left(\frac{L}{2}\right)^2 + R_{ws}^2} - L \approx \frac{2R_{ws}^2}{L}, \quad (14)$$

where we have expanded the expression following the realistic assumption that $R_{ws} \ll L$. Finally, we have

$$\frac{L}{R_{ws}} = \frac{2TR_{ws}}{|E_{pin}|} \sim 10^3, \quad (15)$$

where the standard NS values have been used: T ~20 MeV fm^{-1} (Jones 1990), R_{ws}~30 fm^{-1} and $|E_{pin}|$ ~1MeV. Equation (15) contributes to the dependence and variations of the parameter L.

Using the standard nuclear star values in above Eq (15): T ~20 MeV fm^{-1} (Jones 1990), R_{ws}~30 fm^{-1} and $|E_{pin}|$ ~1MeV. Note that the power of a vortex to bend and adapt to a stapled configuration plays a very important role in determining the most of the effective interaction pinning energy as additionally found by Link [4,22,35].

We tend to finally notice that the selection u =R_{ws} created within the derivation of equation (15) is physically acceptable for a general, order of magnitude definition of vortex rigidity sinceR_{ws} is that the natural length-scale of the system, additionally where pinning is concerned. For example, the pinning energies per site E_{pin} calculated to this point corresponding to the distinction in energy between two configurations (nuclear and interspatial),wherever the vortex has moved by a distance R_{ws}[30-33].Moreover, since $2R_{ws}$ is the average distance between nuclei, displacing a phase of vortex by a distance of the order ofR_{ws} can possibly intersect a new nucleus.

3.Result and Discussion:

3.1. Effective interaction energy persite for nuclear and interspatial pinning inside the neutron star crust:

3.1.1 The effective interaction energy per site E_{in} for Nuclear pinning β=1:

The graph in fig. (4) shows the relation between E_{Pin} and $E_{in}$for the nuclear pinning region. Where E_{Pin} (<0) is pinning energy per pinning site and is given by Eq. (7), $E_{in} = \frac{E_{pin}}{(\alpha+\alpha_0)^2}\left(\alpha^2 + \frac{4}{3}\alpha r_d + \frac{1}{2}{r_d}^2\right)$ where α is the drag parameter, r_d is drag distance covered by captured radius inside the vortex. In the case β=1 i.e., during non-polarized vortex-nucleusinteraction, the pairing gap has a maximum of about 3 MeV, which corresponds to the strong pairing scenario.

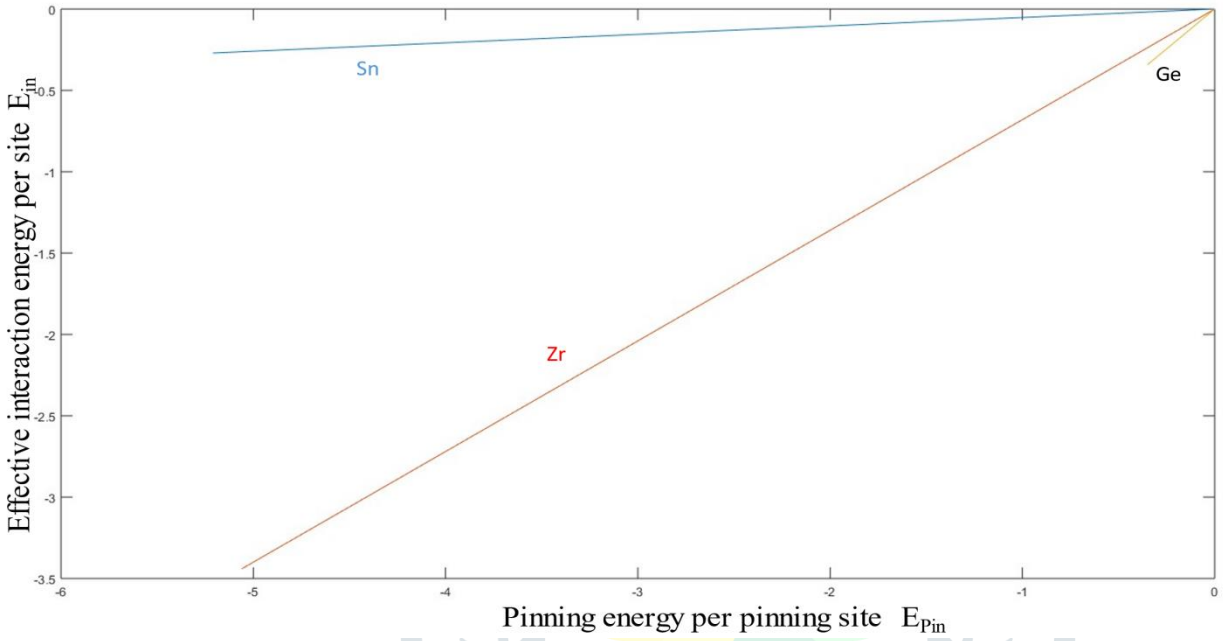

Figure (4): The graph shows the variation in effective pinning energy per pinning site for the three regions ($^{1800}Sn_{50}$, $^{1500}Zr_{40}$, $^{982}Ge_{32}$) of the neutron crust for the condition β=1.

Since in nuclear pinning, the interaction between nuclei and vortices is attractive i.e., nucleus is dragged inside the vortex tube, the pinning energy in these regions ($^{1800}Sn_{50}$, $^{1500}Zr_{40}$, $^{982}Ge_{32}$) is weak due to greater coherence length of superfluid and smaller lattice space of Wigner–Seitz cell radius (R_{ws}). Thus, we obtain negative values of effective interaction pinning energy for these regions. For the region $^{1800}Sn_{50}$different parameters are given by: E_{pin}=-5.21 MeV, $\alpha = 0\ fm$, r_d=7.6 fm the value of $E_{in} = -0.31$ MeV is higher as compared to other two regions. In the region $^{1500}Zr_{40}$, parameters are given by:E_{pin}=-5.06 MeV, $\alpha = 4.6$, r_d=5.7 then the value of $E_{in}$is -3.46 MeVand for $^{982}Ge_{32}$, E_{pin}=-0.35 MeV, $\alpha = 33.6$ fm, r_d=1.1 fm the value of $E_{in} = -0.34\ MeV$. This is because smaller the superfluid coherence length ζ, more will be the pinning inside the pinning regionand sinceα=ζ– R_N, when$\alpha = 0$ for Sn, the value of $E_{in}$for Sn is greater as compared to the other two regions in the graph of fig. (4).

3.1.2. The effective interaction energy per site E_{in} for Nuclear pinning β=3:

Again using Eq. (7) we plot a graph as shown in fig. (5) for β=3 i.e., the one in which the effect of the polarization is maximum indicating that the pairing gap has a maximum of about 1 MeV, as usually assumed in the weak pairing scenario.

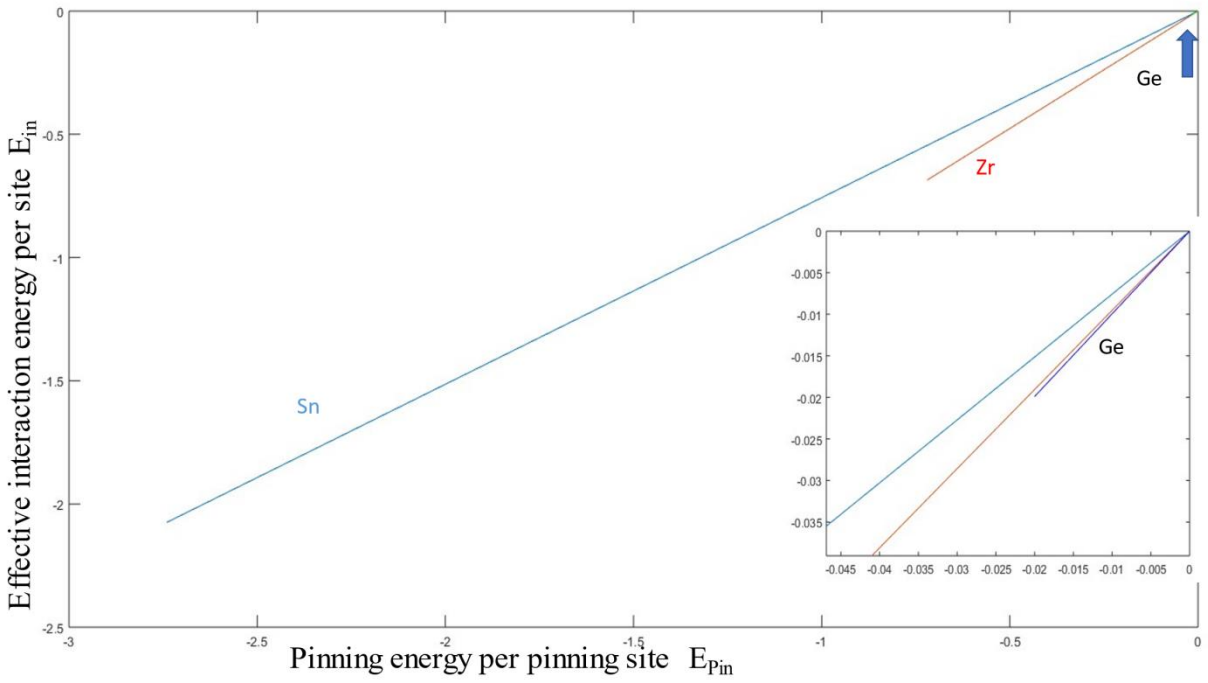

Figure (5): The graph shows the variation in effective pinning energy per pinning site for the three regions ($^{1800}Sn_{50}$, $^{1500}Zr_{40}$, $^{982}Ge_{32}$)when β=3.

So, if we compare the two graphs for β=1 and β=3 we can clearly note the slight increase in the values of E_{in} for the three different regions. In the fig. (5) E_{in}= -0.02 MeVwhen E_{Pin}=-0.02MeV, $\alpha = 111.2\ fm$, r_d=0.3 fmfor Ge (inside the smaller graph with purple line) while E_{in}= -2.08 MeV when E_{Pin}=-2.74 MeV,$\alpha = 8.1\ fm$, r_d=5.5 fm for Sn and E_{in}=-0.69 whenE_{Pin}=-0.72 $\alpha = 26.8\ fm$, r_d=2.1 fmfor Zr-region. Due to the weak pairing gap in β=3 (i.e.,1MeV), nuclei get displaced from its equilibrium position since the lattice has elastic properties and this increases the possibility of pinning hence pinning energy increases slightly in these regions resulting in the increase of values of E_{in}but still the values of E_{in} (<0) are negative as predicted by Negele &Vautherin (1973) and Donati& Pizzochero (2004,2006).

3.1.3. The effective interaction energy per site E_{in} for Interspatial pinning β=1:

In some regions E_{Pin} is positive, i.e., it costs energy to introduce a nucleus in a vortex. In these regions, the vortex–nucleus interaction is repulsive and is known as 'interspatial' pinning (IP). Here the favoured vortex configurations are in-between nuclei. The value of $E_{in}$for Interspatial pinning depends on two conditions i.e., from Eq. (12)

$$E_{in} = \begin{cases} E_{pin}\left(\alpha^2 + \frac{4}{3}\alpha r_d + \frac{1}{2}{r_d}^2\right) r_d \le \alpha \\ E_{pin}\frac{\alpha^2}{6{r_d}^2} \qquad r_d > \alpha \end{cases}$$

The graph in fig. (6) below is for the condition when $r_d \leq \alpha$. It means that the drag distance r_d is smaller than the drag parameter ($\alpha = \zeta + R_N$) resulting an increase in the effective interaction energy E_{in} of thesetwo regions.

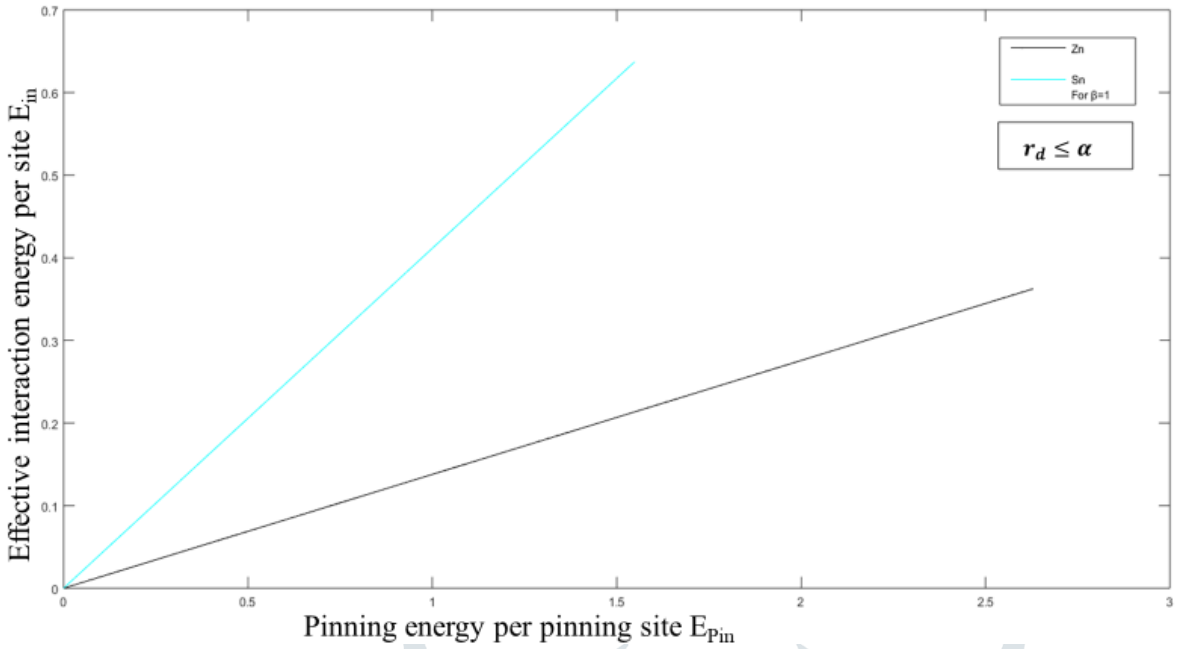

Figure (6): The above graph shows the changes in the effective interaction energy with respect to the pinning energy per site for the two interspatial regions $^{1100}Sn_{50}$ and $^{320}Zr_{40}$ for β=1.

For β=1,$r_d = 14\ fm$, α=14.7 fm then E_{in}=0.64 MeV for Sn region and when r_d=6.2 fm, α=11.1 fm then E_{in}=0.36 MeV for Zr region. The pinning of a nuclei depends upon the drag distance,r_d. Greater the drag distance more will be the pinning inside the vortex of the superfluid. These regions experience more interaction as compared to the other three nuclear pinning regions shown in fig (4) and (5).

Now, let us see the graph for same Eq. (12)in the case of β=3. The polarization causes the weak pairing of nuclei due to which pairing in these regions are less frequent. Since, in interspatial region the interaction is repulsive so, it easily gets dislocated from its equilibrium position under the action of pinning force. In the fig. (7) we can see that when the drag distance is r_d=3.9 fm,α=26 fm, E_{pin}=0.21 MeV then we get E_{in}=0.17 MeV for Zr region (represented by straight line in the fig. 7). For Sn-region we have r_d=2.7 fm, α=19 fm, E_{pin}=0.29 MeV then E_{in}=0.24 MeV. Here, coherence length of the superfluid crust is ζ=20 fm for Zn and ζ=13 fm for Sn, we have explained earlier that for strong pinning, coherence length of the vortex should be smaller than the lattice space of the nuclei. Since, Sn has smaller value of ζ, the pinning in this region will be significantly greater as compared to Zr-region. Resulting an increase in the effective interaction energy E_{in} of Sn-region inside the crust of neutron star.

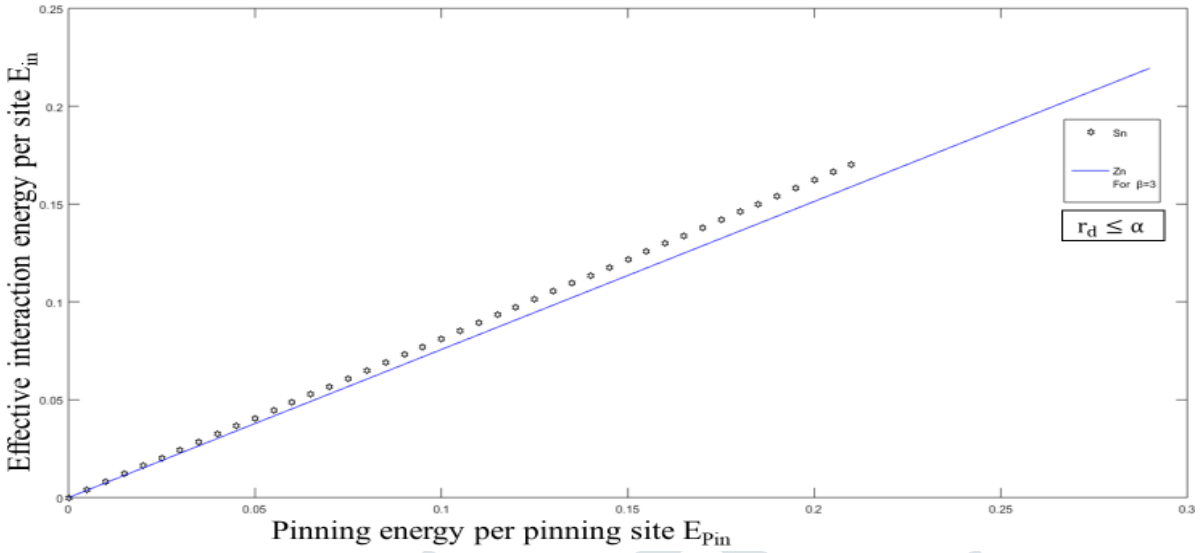

Figure (7): The above graph shows the variation in the effective interaction energy with respect to the pinning energy per site for the two interspatial regions $^{1100}Sn_{50}$ and $^{320}Zr_{40}$ for β=3. Here, straight line represents the Zr-region and star line represents the Sn -region.

3.2. Variation in the radius of nucleus (R_N) with respect to coherence length (ζ) during pinning action:

In this section, we represent the variation in R_N caused by the displacement of nucleus from its equilibrium position during pinning action. When the pinning occurs due to attractive interaction,nucleus is dragged towards the vortex during vortex-nucleus interaction. Since, the interaction is attractive, the captured nucleus depends on the radius of the vortex (ζ) along with the drag distance (r_d) it covers during the pinning action as shown in fig. (1) and then we define the capture radius r_{cap} as the radius within which it is energetically favourable for the nuclei to be displaced. Thus, for nuclear pinning, r_{cap} is defined by Eq. (5) i.e., $r_{cap} = \alpha + r_d = \zeta - R_N + r_d$.

Figure (8): (a) Representation of increase in capture radius for the three regions $^{1100}Sn_{50}$ and $^{320}Zr_{40}$ with respect to coherence length ζ and drag distance r_d for the condition β=1. (b) Representation of increase in capture radius for the three regions $^{1100}Sn_{50}$ and $^{320}Zr_{40}$ with respect to coherence length ζ and drag distance r_d for the condition β=3.

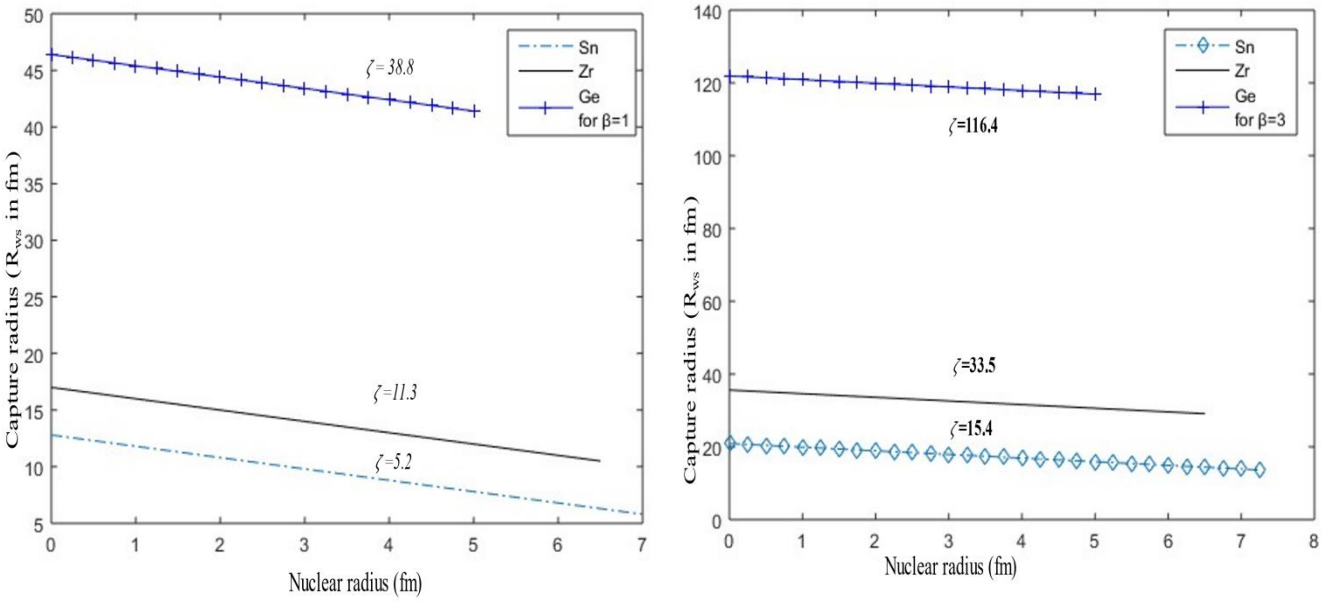

Also, for the region with smaller value of ζ, drag distance (r_d) will be greater since, dragging will be required for vortex-nucleus interaction during the pinning action. Therefore, $^{1100}Sn_{50}$- region will have lowest value of ζ (i.e., ζ=5.2 fm, for β=1 and ζ=15.4 fm, for β=3) and greatest drag distance (r_d=7.6 fm, for β=1 and r_d=5.5 fm, for β=3).

Moreover, the condition β=1 and β=3 shows the sudden increase in capture radius due to ζ for strong and weak pairing of nucleus for 3MeV and 1 MeV pairing gap.

Next, when the vortex-nucleus interaction i.e., when the nucleus is inside the vortex and get expelled instead of getting drag towards the vortex (as shown in fig. 2), the capture radius is given by Eq. (17) i.e., $r_{cap} = \alpha = \zeta - R_N$. In this case, interspatial pinning take place and there is no role of drag distance for defining capture radius because nucleus is already inside the vortex. Fig. (9) represent the value of capture radius which only depends upon the repulsive radius of vortex (or coherence length ζ) undergoing interspatial pinning for $^{1100}Sn_{50}$ and $^{320}Zr_{40}$ regions. In fig. (9.a) when nucleus radius R_N is at 0 fm, r_{cap} and ζ have the same values which shows that capture radius at this point solely depend upon the coherence length of the superfluid. And when β=1 i.e., during strong pairing gap (value of β=1is 3MeV) R_N=6 fm,ζ=6.7 fm for $^{320}Zr_{40}$ the value of r_{cap} is 0.7 fm indicating the decrease in radius capture. Similarly, when β=3, R_N=6 fm, ζ=20 fm the value of r_{cap} is 14 fm which shows the increase in r_{cap} due to weak pairing gap (i.e., value of β=3 is 1MeV).

Figure (9): (a) Representation of decrease in capture radius with respect to coherence length ζ,in$^{320}Zr_{40}$– region for both the condition of

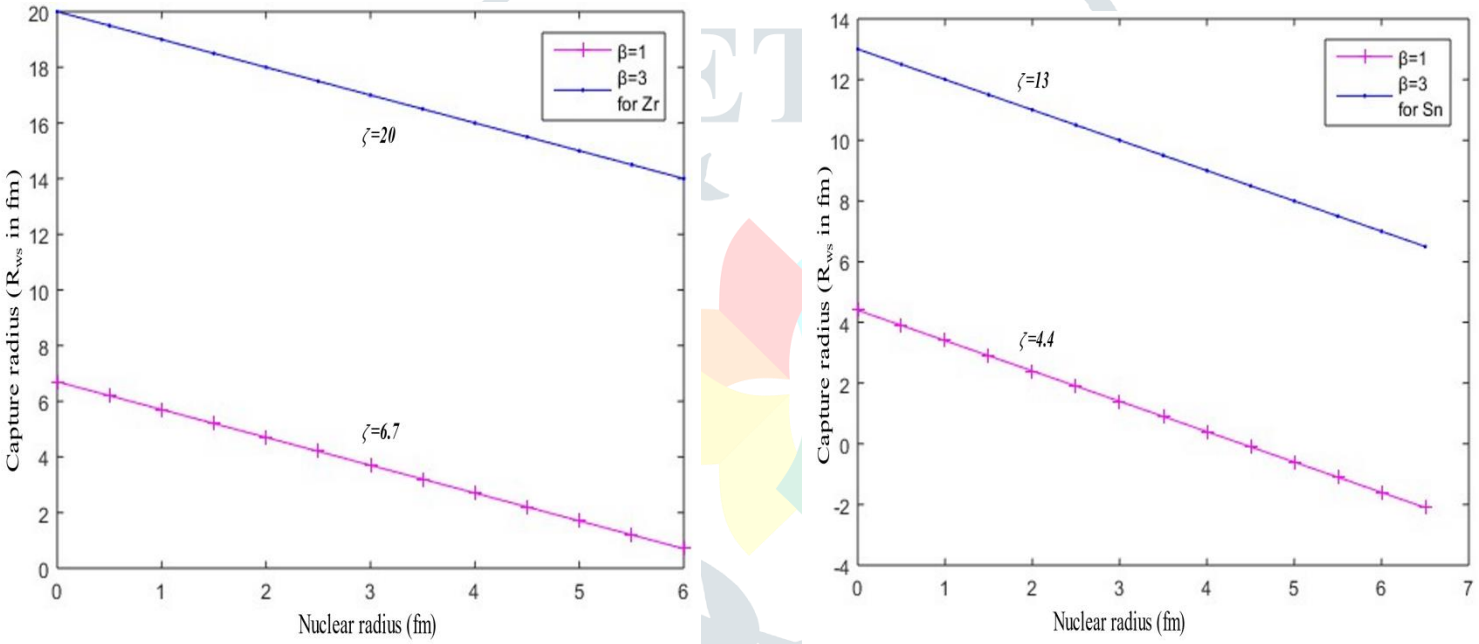

suppression factor β. (b) Representation of decrease in capture radius with respect to coherence length ζ,in$^{1100}Sn_{50}$– region for both the condition of suppression factor β.

For $^{1100}Sn_{50}$ (fig. 9.b), again when nucleus radius R_N is at 0 fm, r_{cap} and ζ,have the same values i.e., again capture radius at this point solely depend upon the coherence length of the superfluid and as the value of R_N increases, r_{cap} decreases. For β=1, whenR_N=6.7fm, ζ, =4.4 fm then the value of r_{cap} is -2.3 fm and for β=3 condition, when R_N=6.7fm, ζ, =13 fm the value of radius capture is 6.3 fm showing yet again a decrease in capture radius. Comparing fig. (8)and fig. (9), we see that interspatial pinning shows the opposite behaviour as compared to nuclear pinning. In nuclear pinning the value of r_{cap} is always greater than R_N for all the three regions whereas, it decreases in case of repulsive pinning.

For the ease of understanding these two-pinning action better, let us take the example of cyclone experiencing Coriolis effect. Cyclone drag the things (e.g.: tree, fishes etc.,) in between its way towards itself from the bottom and then expelled it from where the force is weaker. This attraction and repulsive nature of cyclone can be related to these pinning action of vortex inside the crust of neutronstar. Since, Coriolis force in cyclone include both counter-clockwise and clockwise rotation, the nature of pinning inside vortex-nuclear interaction is somewhat similar to this example.

Finally, we note that our approach relies on calculating energy differences between vortex configuration; therefore, it cannot give any information about the short-range radial profiles of the mesoscopic pinning energies and forces (incidentally, the existing microscopic studies of the vortex–nucleus interaction are also based on energy arguments between specific configurations, giving no information about the short-range radial dependence of the interaction). Dynamical vortex line simulations will thus be necessary to assess the stability of these configurations and how vortices move from one to another. The main difficulties in modelling these phenomena lies in the large separation in scales that exists in neutron stars between the interactions of vortices, flux tubes and clusters on the Fermi scale, vortex-vortex interactions on the scale of millimeters and the large-scale hydrodynamics of the star.

4. Conclusion

This paper explains some basic aspects of the physics of superfluidity in neutron stars like: vortex quantization in superfluid region inside NS crust, the existence of vortices, mechanisms of vortex pinning and finding the expression for effective interaction pinning energy for both nuclear and interspatial pinning in the crust of NS. We now conclude that effective interaction energy for pinning of the nuclei inside vortex depend upon several factors such as coherence length of the superfluid ζ, drag parameter α, drag distance from the equilibrium position r_d, radius of the nuclei R_N, radius of the cell R_{ws}, polarization factor β, pairing gap of the nuclei and the pinning energy per pinning site. From the graphs shown in result section, we find that pinning energy basically depend very less on the whether the pinning is in nuclear or interspatial region but more on the polarization effects, which changes the angular momentum distribution in the NS crust by shifting the positions of nucleus to maximum. Thus, in this paper, we presented the variation in effective interaction energy per pinning sitewhich is further helpful for finding the pinning force per unit length acting on a vortex in an NS crust and showed the dependence of coherence length ζ and drag distance r_d for finding the capture radius r_{cap} for the two pinning actions in BCC lattice.For the other random lattice, the pinning energyE_{Pin} and effective interaction energy E_{Pin}does not vary considerably from the estimates within the BCC case, and depends principally on the average distance between pinning sites, the pinning energy, the coherence length,and rigidity of the vortex, with the precise nature of the lattice solely causative a geometrical issue of order unity. Furthermore, the crust of a NeutronStarmay not be a BCC lattice however might exhibit a lot of heterogeneous structure ormany varieties of ‘pasta’ phases at the crust/core interface, neutering the pure mathematics of the nuclear clusters. We tend to explore in detail the results of those effects on vortex pinning along with the impurities of lattice and tangled vortex nature in future work.

Reference

[1] L. Onsager, “Statistical hydrodynamics,” Il Nuovo Cimento, vol. 6, pp. 279–287, Mar. 1949.
[2]Aurel Bulgac,1 Michael McNeil Forbes,2, 3 and Rishi Sharma4 “Strength of the Vortex-Pinning Interaction from Real-Time Dynamics”
[3] T. Shapoval, V. Metlushko, M. Wolf, B. Holzapfel, V. Neu, and L. Schultz, Phys. Rev. B **81**, 092505 (2010), arXiv:0907.2821 [cond-mat.supr-con].
[4] Link B., Cutler C., 2002, MNRAS, 336, 211
[5] B. Link, R. I. Epstein, and J. M. Lattimer, Phys. Rev. Lett. **83**, 3362 (1999), arXiv:Astroph/9909146.
[6] P. W. Anderson and N. Itoh, Nature **256**, 25 (1975).
[7]N. Andersson, K. Glampedakis, W. C. G. Ho, and C. M. Espinoza, Phys. Rev. Lett. **109**, 241103 (2012), arXiv:1207.0633; N. Chamel, Phys. Rev. Lett. **110**, 011101(2013), arXiv:1210.8177.
[8] Link B., 2012, MNRAS, 422, 1640
[9] J. A. Bowers and K. Rajagopal, Phys. Rev. D **66**, 065002 (2002), arXiv:hep-ph/0204079; M. Mannarelli, K. Rajagopal, and R. Sharma, ibid. **76**, 074026 (2007), arXiv:hepph/ 0702021 [hep-ph]
[10] S. Tung, V. Schweikhard, and E. A. Cornell, Phys. Rev. Lett. **97**, 240402 (2006), arXiv: cond-mat/0607697.
[11] Espinoza C. M., Lyne A. G., Stappers B. W., Kramer M., 2011, MNRAS,414, 1679

[12] Baym G., Pethick C., Pines D., Ruderman M., 1969, Nature, 224, 872
[13]Anderson P. W., Itoh N., 1975, Nature, 256, 25
[14] Alpar M. A., 1977, ApJ, 213, 527
[15] Alpar M. A., Pines D., Anderson P. W., Shaham J., 1984a, ApJ, 276, 325
[16] Alpar M. A., Anderson P. W., Pines D., Shaham J., 1984b, ApJ, 278, 791
[17] Alpar M. A., Chau H. F., Cheng K. S., Pines D., 1994, ApJ, 427, L29
[18] Alpar M. A., Chau H. F., Cheng K. S., Pines D., 1996, ApJ, 459, 706.
[19] Alpar M. A., 1977, ApJ, 213, 527
[20] Jones P. B., 1990, MNRAS, 243, 257
[21] Jones P. B., 1991, ApJ, 373, 208
[22] Hirasawa M., Shibazaki N., 2001, ApJ, 563, 267
[23]S. Seveso, P. M. Pizzochero,F. Grilland B. Haskell, 2016,Mon. Not. Roy. Astr. Soc., 455, 3952
[24] Link B., 2014, MNRAS, 789, 141
[25] D. V. Osborne, "The Rotation of Liquid Helium II," Proceedings of the Physical Society. Section A, vol. 63, pp. 909–912, Aug. 1950.
[26] L. Onsager, "Statistical hydrodynamics," Il Nuovo Cimento, vol. 6, pp. 279–287, Mar. 1949.
[27] R. P. Feynman, Application of Quantum Mechanics to Liquid Helium. Progress in Low Temperature Physics, vol. 1. Amsterdam: North-Holland, 1955
[28] Vanessa Graber, thesis:'Cosmic, condensates vortex, fluxtube and Nuclear Star dynamics.'
[29] A. A. Abrikosov, "The magnetic properties of superconducting alloys," Journal of Physics and Chemistry of Solids, vol. 2, pp. 199–208, Jan. 1957.
[30] Donati P., Pizzochero P. M., 2003, Phys. Rev. Lett., 90, 21
[31] Donati P., Pizzochero P. M., 2004, Nucl. Phys. A, 742, 363
[32] Donati P., Pizzochero P. M., 2006, Phys. Lett. B, 640, 74
[33] Hirasawa M., Shibazaki N., 2001, ApJ, 563, 267
[34] Gandolfi S., Illarionov A. Yu., Fantoni S., Pederiva F., Schmidt K. E., 2008, Phys. Rev. Lett., 101, 132501
[35] Link B., 2009, Phys. Rev. Lett., 102, 131101
[36] Chamel N., 2013, Phys. Rev. Lett., 110, 011101
[37] Kobyakov D., Pethick C., 2014, Phys. Rev. Lett., 112, 112504
[38] Piekarewicz J., Fattoyev F. J., Horowitz C. J., 2014, Phys. Rev. C, 90, 015803
[39] Pizzochero P. M., 2011, ApJ, 743, L20
[40] Fetter A. L., 1967, Phys. Rev. D, 4, 1589
[41] Haskell B., Melatos A., 2015a, International J.ModernPhy. D, 24, 1530008
[42] Haskell B., Melatos A., 2015b, MNRAS, submitted, preprint
[43] Haskell B., Pizzochero P. M., Sidery T., 2012, MNRAS, 420, 658
[44] Haskell B., Pizzochero P. M., Seveso S., 2013, ApJ, 746 L25
[45] Haskell B., Antonopoulou D., 2014, MNRAS, 438, L16
[46] H. Kojima, W. Veith, S. Putterman, E. Guyon, and I. Rudnick, "Vortex-Free Landau State in Rotating Superfluid Helium," Physical Review Letters, vol. 27, pp. 714–718, Sept. 1971.
[47] Migdal A. B., 1959, ApJ, 743, L20;2 Ginzburg and Kirzhnits, 1965
[48] Negele J. W., Vautherin D., 1973, Nucl. Phys. A, 207, 298
[49] Seveso S., Pizzochero P. M., Haskell B., 2012, MNRAS, 427, 1089
[50] Radhakrishnan and Manchester, 1969; Reichley and Downs, 1969